Title

Adaptive synergy between catechol and lysine promotes wet adhesion by surface salt displacement

Journal

Science, 349(6248)

ISSN

0036-8075 1095-9203

Authors

Maier, G. P
Rapp, M. V
Waite, J. H
et al.

Publication Date

2015-08-06

DOI

10.1126/science.aab0556

Science, 2015, *349*, 628-632. DOI: 10.1126/science.aab0556

Adaptive synergy between catechol and lysine promotes wet adhesion by surface salt displacement

Greg P. Maier,[1†] Michael V. Rapp,[2†] J. Herbert Waite,[3*] Jacob N. Israelachvili,[2,4*] Alison Butler[1*]

[1]Department of Chemistry and Biochemistry, University of California, Santa Barbara, California 93106, USA.
[2]Department of Chemical Engineering, University of California, Santa Barbara, California 93106, USA.
[3]Molecular, Cellular, and Developmental Biology, University of California, Santa Barbara, California 93106, USA.
[4]Materials Department, University of California, Santa Barbara, California 93106, USA.

*Correspondence to herbert.waite@lifesci.ucsb.edu; jacob@engineering.ucsb.edu; butler@chem.ucsb.edu.

†These authors contributed equally to this work.

One Sentence Summary: Siderophore-inspired, mussel foot protein mimetic adhesives resist oxidation and reveal a synergistic catechol-lysine interplay that enables wet adhesion to mineral surfaces

Abstract: In physiological fluids and seawater, adhesion of synthetic polymers to solid surfaces is severely limited by high salt, pH, and hydration, yet these conditions have not deterred the evolution of effective adhesion by mussels. Mussel foot proteins provide insights about adhesive adaptations: notably, the abundance and proximity of catecholic Dopa (3,4-dihydroxyphenylalanine) and lysine residues hint at a synergistic interplay in adhesion. Certain siderophores—bacterial iron-chelators—consist of paired catechol and lysine functionalities thereby providing a convenient experimental platform to explore molecular synergies in bioadhesion. These siderophores and synthetic analogs exhibit robust adhesion ($W_{adh} \geq 15 mJ/m^2$) to mica in saline pH 3.5-7.5 and resist oxidation. The adjacent catechol-Lys placement provides a "1-2 punch", whereby Lys evicts hydrated cations from the mineral surface, allowing catechol binding to underlying oxides.

Water disrupts adhesion on polar surfaces by forming hydration layers that impede intimate contact between adhesive polymers and surfaces. Sessile marine organisms, including barnacles, kelps, and mussels, routinely adhere to wet saline surfaces, suggesting that successful adaptations for removing weak boundary layers have evolved. Identifying these adaptations holds great promise for adhesion science and technology. The mussel holdfast or byssus contains ~15 adhesive mussel foot proteins (mfps), two of which, mfp-3 and mfp-5, are deposited first as a primer to condition the target surface and enable other mussel foot proteins to adhere (*1*) and are peculiar in containing between 20-30 mol% Dopa. Demonstration by atomic force microscopy of wet adhesion to titania by a single Dopa (*2*) sparked functionalization of synthetic polymeric adhesives and self-healing hydrogels with catechol (*3*–*8*), but wet adhesion of these polymers to oxides and minerals remains controversial (*9*, *10*). In actuality, mfp-3 and -5 are rich in Lys as well as Dopa —frequently in adjacent positions along the protein backbone (*1*). The surface forces apparatus (SFA) has measured impressive wet adhesion of these proteins to mineral, oxide, and organic surfaces (*11*). Dopa residues in mfp-3 and -5 form bidentate coordination and hydrogen bonds to mineral and oxide surfaces, and hydrophobic interactions on polymeric surfaces (*11*), but only if protected from oxidation by low pH and anti-oxidants during deposition (*12*, *13*). Several mimics of mussel foot proteins have been synthesized, most notably Dopa-Lys copolymers by Yamamoto (*14*) and Deming (*15*) using N-carboxyanhydride ring opening polymerization, as well as the polymer brush anchors developed by Messersmith (*6*). However, the role of Lys in both the mussel surface primers and in synthetic wet adhesives remains poorly understood.

Many marine and pathogenic bacteria have evolved an adaptive iron-sequestration pathway that is based on catechol-containing siderophores, including enterobactin, the cyclic

lactone of *tris*-2,3-dihydroxybenzoyl-L-Ser (2,3-DHBA-L-Ser) (*16*). The plant pathogen *Dickeya chrysanthemi* produces the siderophore, cyclic trichrysobactin (CTC), the lactone of *tris*-2,3-DHBA-D-Lys-L-Ser (Fig. 1A) in which Lys is present adjacent to each catechol (*17*). The prominence and proximity of catechol and Lys in CTC resemble the interfacial adhesive proteins mfp-3 and mfp-5. However, the mass of CTC (1053 g/mol) is a fraction of the mfp-3 and 5 masses (6kDa and 10kDa, respectively). As such, the siderophore has relaxed steric constraints when adsorbed to a surface, and the simpler siderophore structure allows for more straightforward interpretation of the adhesive mechanisms. In addition, the autoxidation of 2,3-DHBA is much slower than 4-methylcatechol, a proxy for the 3,4-dihydroxy substituents in the Dopa catechol, at pH 7.5 and 10 (Fig. S1 and Supplementary Text), reflecting intramolecular H-bonding between the ortho-OH and the carbonyl oxygen, and the electron withdrawing nature of the carboxylate substituent (Fig. 1B), both of which stabilize CTC against oxidation compared to Dopa in mussel foot proteins. Ultimately, the subtle molecular differences make 2,3-DHBA in siderophores significantly more oxidation resistant and enlarge the pH range over which these compounds bind to target surfaces.

A surface forces apparatus (SFA) was used to measure the normalized force (F/R)-distance (D) profiles of two molecularly-smooth mica surfaces (of radius R) during their approach and separation in buffered solutions of CTC (*18*). In these SFA measurements, the surfaces are first slowly brought into contact and compressed. The thickness of the intervening compressed film between the surfaces is measured as D_T. The surfaces are then slowly separated and the adhesion force (F_{ad}/R) is measured at the force minimum, at a point just before the surfaces rapidly jump apart.

Mica is an anionic and molecularly smooth aluminosilicate mineral that allows for Å-level mechanistic insight during adhesion measurements. In saline solutions, mica adsorbs cations (particularly K^+) to form a tightly bound hydration layer at the solid-liquid interface (*19*, *20*). These hydration layers—present at virtually all marine and physiological interfaces—impose a significant molecular barrier to coatings and high-performance adhesives for wet surfaces (*21*). The effects of these hydration layers between mica surfaces in buffered solution without any added siderophores (Fig. 1C, black circles) are seen in the SFA measurements: when compressed to 10 mN m^{-1}, hydrated K^+ ions form a D_T=13 ± 1 Å thick bilayer between the mica surfaces, and only a weak adhesion force is measured on separation. However, nanomole amounts of CTC form a single monolayer "molecular bridge" that results in a large adhesion force between the micas presumably by displacing the hydrated salt ions from the mica surface (Fig. 1C, red circles). After injecting 10 nanomoles of CTC into the buffered gap solution between the mica surfaces (~50 μL total volume, 200 μM bulk concentration), the compressed film thins to 11 ± 1 Å—indicating that the hydrated salt ions have been replaced with CTC at the surface—and the adhesion force between the surfaces increases ~30-fold to -30 ± 10 mN m^{-1}. As the surfaces are separated, the sharply vertical shape of the separation force curve does not exhibit any observable bridging (i.e., an increase in the separation distance), indicating that the physical bonds supporting adhesion are specific and short-ranged (effective only over several Å), such as a hydrogen bond or specific Coulombic interaction (*20*).

The natural 2,3-DHBA-containing CTC siderophore promotes adhesion at near-neutral pH (pH 6.7), a solution condition that rapidly oxidizes Dopa in mussel foot proteins leading to reduced adhesion (*12*). Yet, the triserine lactone scaffold of CTC hydrolyses under acidic conditions, limiting its usefulness as an adhesive primer over a wide range of pH. To circumvent

this limitation, we synthesized a mimic of CTC, Tren-Lys-Cam (TLC, Fig. 2A) built on the robust tris(2-aminoethyl)amine (Tren) scaffold that retains integrity over a wide pH range (Fig. S2) (*22*). TLC exhibits nearly identical adsorption and adhesion behavior to the natural CTC siderophore. In parallel SFA experiments at pH 3.3 (Fig. 2B), TLC molecules displace hydrated salt ions at the mica surface and, after compression of the surfaces, form a 9 ± 1 Å thick monolayer that bridges between the two surfaces. The thickness of the TLC film, the shape of the force-distance profile (narrow adhesion well), and dramatically increased adhesion all indicate that the synthetic TLC performs similarly to CTC at mineral surfaces.

TLC mediates adhesion between mineral surfaces in saline solution from pH 3.3-7.5 (Fig. 2C). The TLC peak adhesion concentration is ~20 μM (Fig. S3). Adhesion forces measured in SFA experiments are converted to adhesion energies through the Johnson-Kendal-Roberts theory of adhesive surfaces ($E_{ad} = F_{ad}/1.5\pi R$) (*23*). Adhesion is strongest at pH 3.3, and is not statistically different from pH 5.5 for a p-value ≤ 0.05 (Table S1). At pH 7.5, adhesion decreases ($p \leq 0.05$), yet TLC still maintains ~65% of the peak adhesion. The cause for the decrease in adhesion at pH 7.5 is under investigation; we speculate that either slow TLC oxidation or subtle interfacial pH changes reduce the number of bridging hydrogen bonds at pH 7.5. Moreover, adhesion energy increases with contact time before separation—a common trait among adhesives. As longer contact allows for better interfacial equilibration, more siderophore molecules are able to rearrange and maximize the number of bridging bonds (*20*).

To ascertain specific contributions made by catechol and Lys in the siderophore adhesive platform, we synthesized a suite of five additional Tren-based homologs, varying properties of the amine and the aromatic functionalities (Figs. 3A-G, Figs. S4-S13, Tables S2-S4). Group I homologs retain both catechol and amine functionalities (Figs 3B and 3C); Group II retains Lys

but removes the catechol functionality (Figs 3D and 3E); and Group III retains catechol but removes the amine functionality (Figs 3F and 3G). Collectively, the results of the six synthetic homologs reveal a requirement for catechol and an alkylamine cation (e.g. Lys, Dab) for appreciable surface binding and adhesion.

Group I includes TLC and Tren-Dab-Cam (TDC), with the Lys chain shortened by two methylene units to diaminobutyric acid (Dab). Group I assesses whether the length or flexibility of the amine is critical to adsorption and adhesion. The length of the amine chain between 2 to 4 carbons does not alter the homolog's behavior, as both TLC and TDC displace salt on the mica surface and promote large adhesion energies (Figs. 3H-I, Fig. S14C).

Group II homologs test the effect of removing catechol, while maintaining the 4+ cationic charge: Tren-Lys-Pam (TLC) retains one-hydroxyl group, whereas Tren-Lys-Bam (TLB) removes both hydroxyls. Without catechol, the Group II homologs exhibit comparatively weak adhesion between mica surfaces, i.e. ~15% of the Group I homologs with both Lys and catechol. Contrary to the narrow adhesion wells of the Group I homologs, the separation force curves of Group II homologs display weak bridging (~5-10 Å) before the surfaces jump apart (Fig. S14A,B), suggesting that the adhesion may be due to non-specific interactions between 2 or more homologs (such as hydrophobic interactions or π-cation interactions) (*24*). TLB is unable to donate H-bonds and has increased hydrophobicity hence has an increased energy barrier for adsorption; TLP adsorbs to the mica surface at 20 μM (the same as the TLC critical aggregation concentration), yet TLB requires an elevated bulk concentration of 200 μM before adsorption begins.

Group III homologs compromise the amine functionality, through acetylation (Tren-Lys^{Ac}-Cam, TL^{Ac}C) or by omission of Lys (Tren-Cam, TC), while maintaining the catechol

presence. Over the concentration range of 2-200 μM, Group III homologs do not adsorb on the mica surface at high salt (μ =200 mM) and provide no adhesion (Fig. S15A,B). In pure water, TC adsorbs as a multilayer on mica and demonstrates modest cohesion (Fig. S15C).

In sum, the amine and catechol moieties interact synergistically to mediate surface priming by the catechol alkylamine compounds to mineral surfaces. Bidentate catechol-mediated H-bonding is necessary for robust bridging attachments between surfaces, however, catechols alone are insufficient to breach the hydrated salt layer on mica, which is typical of a wide variety of aluminosilicate minerals in its cation binding properties (*25*). The amines in CTC and TLC may serve as molecular vanguards to displace hydrated salt ions and ready the surface for bidentate catechol binding (*26*).

The discovery that 2,3-dihydroxycatechol and alkyl ammonium (e.g., Lys and Dab) functionalities limit oxidation and promote adhesion has relevance to other adhesive platforms in providing a compelling rationale for the >20 mole% of cationic residues in Dopa-rich mussel foot proteins (1) and establishing a set of design parameters for future bio-inspired synthetic polymers. As many synthetic adhesives are functionalized with catechols and amines (27) for improved solubility (10) or cross-linking effects (28, 29), our results highlight the need to couple catechol and cationic functionalities to displace surface salts.

References and Notes:

Reference for Supplementary Information: *(30)*

1. B. P. Lee, P. B. Messersmith, J. N. Israelachvili, J. H. Waite, *Annu. Rev. Mater. Res.* **41**, 99–132 (2011).

2. H. Lee, N. F. Scherer, P. B. Messersmith, *Proc. Natl. Acad. Sci. U. S. A.* **103**, 12999–13003 (2006).

3. M. Krogsgaard, M. A. Behrens, J. S. Pedersen, H. Birkedal, *Biomacromolecules*. **14**, 297–301 (2013).

4. H. Shao, R. J. Stewart, *Adv. Mater.* **22**, 729–733 (2010).

5. C. J. Kastrup *et al.*, *Proc. Natl. Acad. Sci. U. S. A.* **109**, 21444–21449 (2012).

6. A. R. Statz, R. J. Meagher, A. E. Barron, P. B. Messersmith, *J. Am. Chem. Soc.* **127**, 7972–7973 (2005).

7. J. Ryu, S. H. Ku, H. Lee, C. B. Park, *Adv. Funct. Mater.* **20**, 2132–2139 (2010).

8. J. D. White, J. J. Wilker, *Macromolecules*. **44**, 5085–5088 (2011).

9. Y. Li, M. Qin, Y. Li, Y. Cao, W. Wang, *Langmuir*. **30**, 4358–4366 (2014).

10. J. Wang *et al.*, *Adv. Mater.* **20**, 3872–3876 (2008).

11. J. Yu *et al.*, *Proc. Natl. Acad. Sci. U. S. A.* **110**, 15680–15685 (2013).

12. J. Yu *et al.*, *Nat. Chem. Biol.* **7**, 588–590 (2011).

13. N. R. Martinez Rodriguez, S. Das, Y. Kaufman, J. N. Israelachvili, J. H. Waite, *Biofouling*. **31**, 221–227 (2015).

14. H. Yamamoto, *J. Chem. Soc. Perkin Trans. 1*, 613–618 (1987).

15. M. Yu, J. Hwang, T. Deming, *J. Am. Chem. Soc.* **121**, 5825–5826 (1999).

16. K. N. Raymond, E. A. Dertz, S. S. Kim, *Proc. Natl. Acad. Sci. U. S. A.* **100**, 3584–3588 (2003).

17. M. Sandy, A. Butler, *J. Nat. Prod.* **74**, 1207–1212 (2011).

18. J. Israelachvili *et al.*, *Reports Prog. Phys.* **73**, 036601 (2010).

19. R. M. Pashley, *Adv. Colloid Interface Sci.* **16**, 57–62 (1982).

20. J. N. Israelachvili, *Intermolecular and Surface Forces: Revised Third Edition* (Academic Press, 2011).

21. J. Israelachvili, H. Wennerström, *Nature*. **379**, 219–225 (1996).

22. S. J. Rodgers, C. W. Lee, C. Y. Ng, K. N. Raymond, *Inorg. Chem.* **26**, 1622–1625 (1987).

23. K. L. Johnson, K. Kendall, A. D. Roberts, *Proc. R. Soc. A Math. Phys. Eng. Sci.* **324**, 301–313 (1971).

24. S. Kim *et al.*, *J. Mater. Chem. B*. **3**, 738–743 (2014).

25. W. Stumm, J. J. Morgan, *Aquatic Chemistry: Chemical Equilibria and Rates in Natural Waters, 3rd Edition* (John Wiley & Sons, 1996).

26. Y. Akdogan *et al.*, *Angew. Chemie*. **126**, 11435–11438 (2014).

27. P. Podsiadlo, Z. Liu, D. Paterson, P. B. Messersmith, N. A. Kotov, *Adv. Mater.* **19**, 949–955 (2007).

28. F. Zhang, S. Liu, Y. Zhang, Y. Wei, J. Xu, *RSC Adv.* **2**, 8919–8921 (2012).

29. Q. Wei *et al.*, *Angew. Chem. Int. Ed. Engl.* **53**, 11650–11655 (2014).

30. C. Lu, J. Buyer, J. Okonya, M. Miller, *Biometals*. **9**, 377–383 (1996).

Acknowledgments: G.P. Maier and M.V. Rapp contributed equally to this work. We are grateful for support from Materials Research and Science Engineering Centers Program of the National Science Foundation under award DMR 1121053, NSF CHE-1411942 (AB), and NSF GRFP (MR).

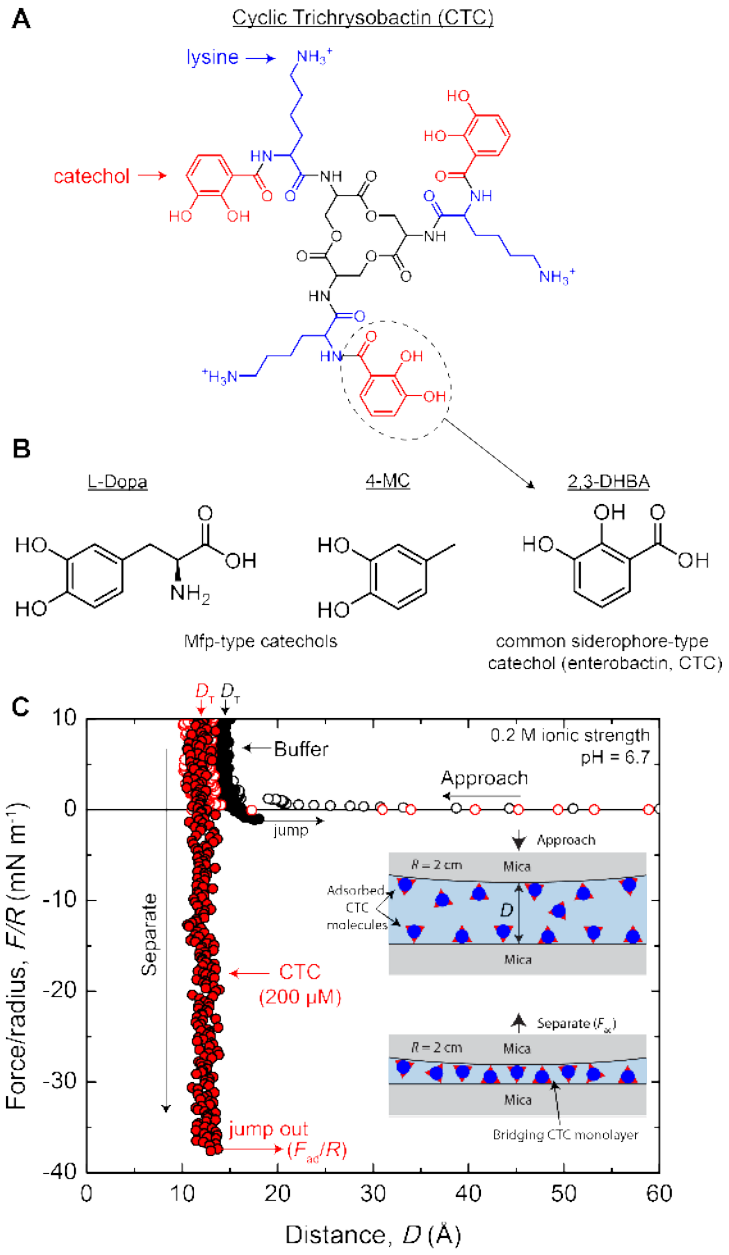

Fig. 1. Adhesion of a natural bacterial catechol siderophore. A, Structure of cyclic trichrysobactin (CTC). B, Structures of catechols illustrating the difference between 3,4-dihydroxy catechol as in Dopa or 4-methylcatechol (4-MC), and 2,3-dihydroxy catechol, as commonly present in 2,3-dihydroxybenzoic acid (DHBA)-containing-siderophores. C, SFA force-distance interaction for CTC-mediated adhesion between two mica surfaces in buffer (50 mM phosphate buffer + 150 mM KNO3) at pH 6.7. The surfaces were left in contact for 30 min before separation. The open and solid circles are for data measured on approach and separation, respectively, of the mica surfaces. The inset displays a schematic of the interacting surfaces throughout the SFA experiments.

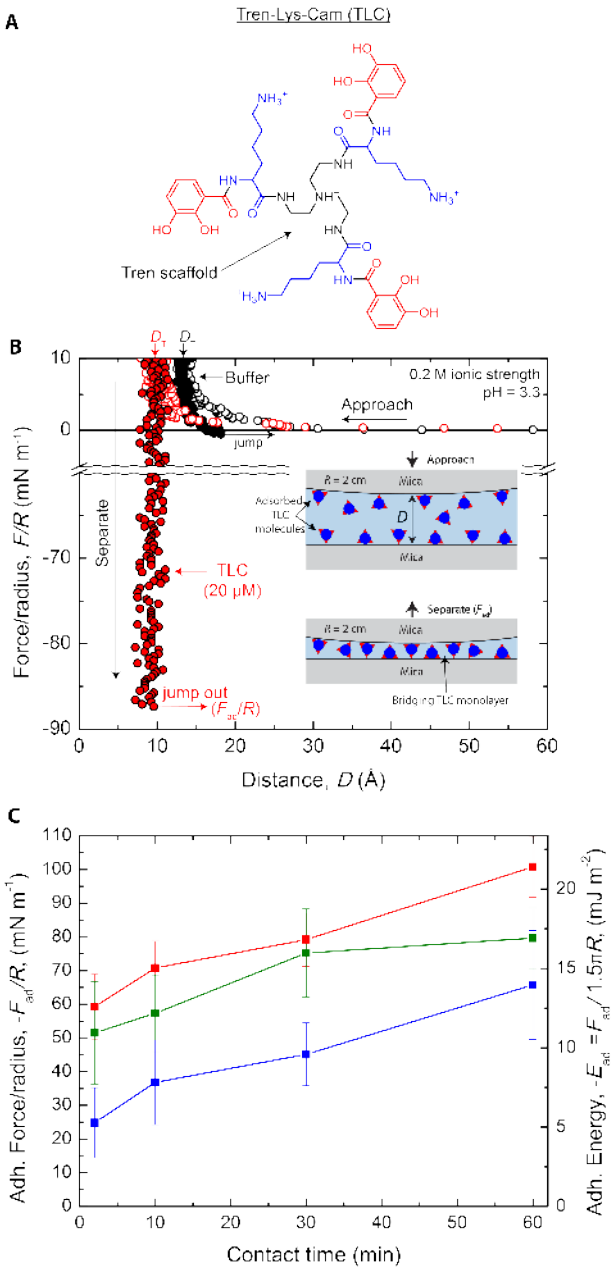

Fig. 2. Adhesion of a synthetic siderophore mimic. A, Structure of Tren-Lys-Cam (TLC), a synthetic mimic of the natural siderophore cyclic trichrysobactin. B, SFA force-distance interaction for the TLC-mediated adhesion between two mica surfaces in buffer (50 mM acetate buffer + 150 mM KNO3) at pH 3.3. The surfaces were left in contact for 30 min before separation. The open and solid circles are for data measured on approach and separation, respectively, of the mica surfaces. The inset displays a schematic of the interacting surfaces throughout the SFA experiments. C, The adhesive force (and energy) required to separate two mica surfaces adsorbed with 1-10 nmoles (20-200 μM) of TLC, as a function of both the time the mica surfaces were left in contact and the buffer solution pH. Error bars (± 12 mN m-1) for the pH 3.3 and 5.5 measurements have been omitted for visual clarity.

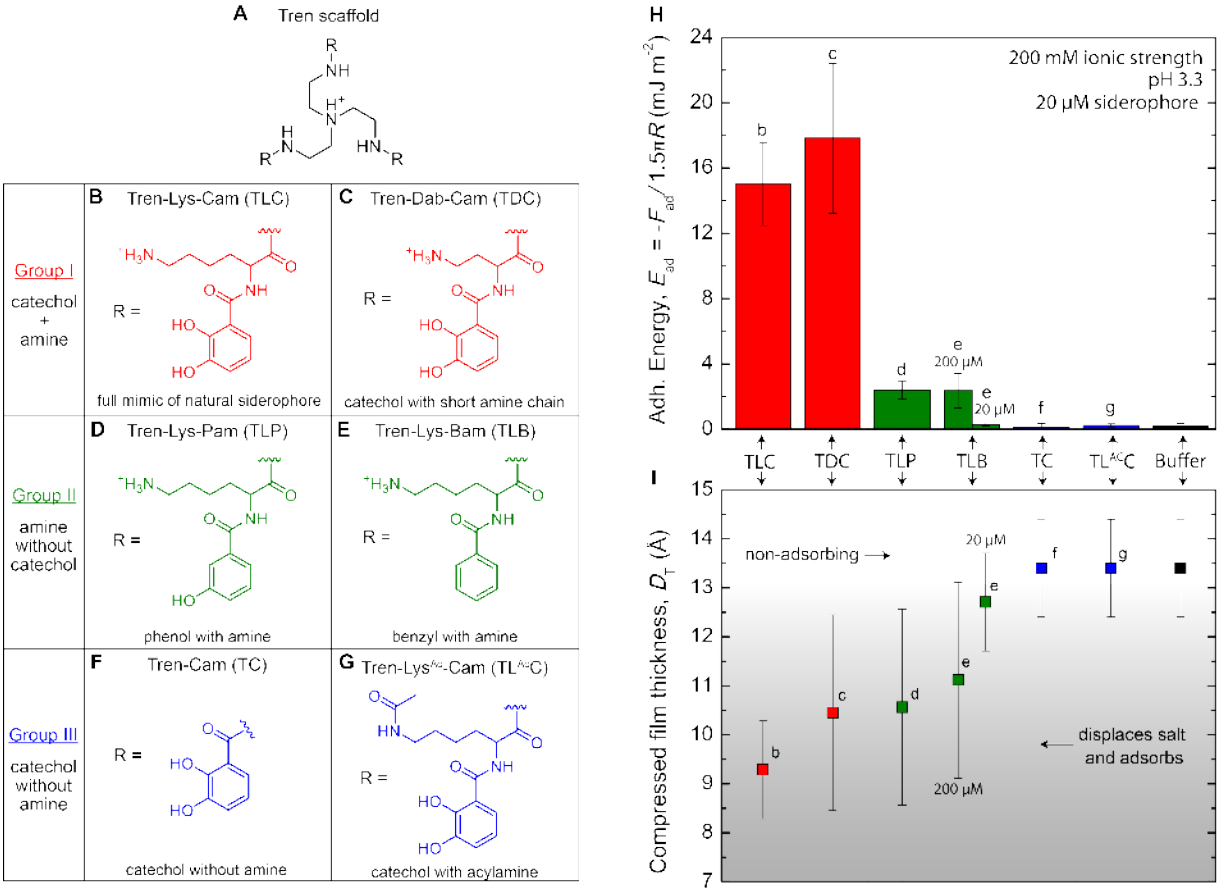

Fig. 3. The synergy of catechol and Lys in siderophore adhesion. A, Structure of the Tren scaffold. B-G, the R groups appended to Tren. H, The average adhesion energy required to separate two mica surfaces adsorbed with 1 nmole (20 μM) of the homolog in buffer (50 mM acetate + 150 mM KNO_3) at pH 3.3 after 10 minutes of contact. I, The average film thickness, D_T, of the siderophore monolayer between two mica surfaces at 10 mN/m of compressive load. The film thicknesses correspond with the adhesion energy displayed in H, above. A decreased film thickness (<12 Å) indicates that homologs B, C, D, and E (200 μM) adsorb, displace hydrated salt at the mica surface, and mediate adhesion between two mica surfaces. SFA force-distance measurements for each molecule are shown in Figs. S14-S15.

Supplementary Materials:

Materials and Methods

Supplementary Text

Figures S1-S15

Tables S1-S4